7th International Conference on Debris-Flow Hazards Mitigation

Optical measurements of velocity and of solid volume fraction in fast dry granular flows in a rectangular chute

L. Sarno[a,*], L. Carleo[a], M. N. Papa[a], P. Villani[a,b]

[a]*Department of Civil Engineering, University of Salerno, Via Giovanni Paolo II, 132, 84084 Fisciano, Italy*
[b]*CUGRI, University Consortium for Research on Major Hazards, Salerno, Italy*

Abstract

Geophysical flows, like avalanches and debris flows, are characterized by the gravity-driven motion of a granular medium immersed in an interstitial fluid. To better understand their dynamics, laboratory investigations represent invaluable tools and are essential to study several peculiar features (e.g. the effects of fixed boundaries, non-local momentum exchanges, segregation effects) that are difficult to isolate at the field scale. An experimental study on dry granular flows in a chute geometry is reported. Different basal conditions are investigated by varying the bed roughness. Several flow rates are investigated by adjusting the inflow boundary condition. By employing two high-speed cameras and particle image velocimetry (PIV) technique, accurate velocity measurements (typical error ≈0.004 m/s) could be obtained at sidewall and free surface. An innovative stochastic-optical method [Sarno et al., Granul. Matter, 2016], which exploits highly controlled illumination conditions guaranteed by a flickering-free planar lamp, allowed to obtain reliable volume fraction profiles (typical error ≈0.025). The method uses a transfer function, numerically determined on random grain distributions of known volume fraction. This function stochastically relates the near-wall volume fraction with a measurable quantity, named *two-dimensional volume fraction* and accessible by binarization of digital pictures, taken by a high-speed camera. The combined knowledge of velocity and volume fraction fields allowed a detailed description of the rheological behavior of channelized granular flows and of the effects of the flume boundaries. The superposition of different flow regimes is revealed by different shapes of velocity and volume fraction profiles along the flow depth. It emerges that frictional momentum exchanges increase at the expense of collisional mechanisms with increasing depth. This behavior appears related to the sidewall resistances and to the increasing normal pressures.

Keywords: granular flows; volume fraction; sidewall friction; boundary conditions; rheological stratification.

1. Introduction

Granular materials are ubiquitously involved in hazardous geophysical phenomena, such as debris flows and avalanches. Yet, to date several aspects of their dynamics remain not completely understood. Beside theoretical and field-scale investigations (e.g. Iverson and Vallance, 2001; Medina et al., 2008; Kuo et al., 2009; Iverson and George, 2014; Sarno et al., 2017; Papa et al., 2018), laboratory experiments on granular media still represent an extraordinary tool to get insight into the granular dynamics (e.g. GDR Midi, 2004; Sarno et al., 2011a; Baker et al., 2016; Sarno et al., 2018a). Granular flows exhibit a rich variety of flow regimes, ranging from a *solid-like* behavior in the case of slow deformations and frictional dissipation mechanisms to a *gas-like* behavior in the case of large deformations and strong collisions among grains. An intermediate regime, frequent in geophysical flows and known as *dense-collisional*, is characterized by the coexistence of collisional and frictional mechanisms. To date, a unified constitutive law capable of reliably describing all these flow regimes is lacking. Moreover, some peculiarities of the granular dynamics, such as the effects of fixed boundaries (e.g. Jop et al., 2005; Sarno et al., 2011b), the occurrence of a rheological stratification (e.g. Armanini et al., 2005; Sarno et al., 2014) and non-local momentum exchange mechanisms (e.g. Mills et al., 1999; Pouliquen and Forterre, 2009) still require efforts to be properly described.

The flow velocity and solid volume fraction fields represent crucial quantities to be investigated in laboratory. In particular, the volume fraction is coupled with the rheological behavior of the granular medium in free-surface flows where a stress-free boundary condition occurs at the free surface. While optical techniques for measuring the flow

* Corresponding author e-mail address*: lsarno@unisa.it*

velocity (e.g. particle image velocimetry, PIV, and particle tracking velocimetry, PTV) have reached a certain maturity (e.g. Jesuthasan et al., 2006; Sarno et al., 2018b), the reliable estimation of the volume fraction is much more challenging. For obtaining reliable velocity measurements, in the present work we employed a multi-pass PIV approach (Sarno et al., 2018b) by using the open-source code PIVlab (Thielicke and stamhuis, 2014). Conversely, the stochastic-optical method (SOM) by Sarno et al. (2016) is employed for estimating the sidewall volume fraction.

We present an extensive experimental campaign on steady dry granular chute flows with various basal surfaces. Sarno et al. (2018a) recently reported an investigation on chute flows with chute inclination angle of 30°, where a rich variety of velocity profiles, depending on the roughness of the basal surface and also on the flow depth, was observed. As an extension of the work by Sarno et al. (2018a), here we report new experiments, performed with the same apparatus but with the higher chute inclination angle of 35°. Moreover, different from Sarno et al. (2018a), we obtained not only the velocity measurements but also reliable measurements of the sidewall volume fraction, which are particularly useful for better understanding the granular flow dynamics. The employment of several bed surfaces allowed to investigate different basal kinematic boundary conditions (KBC): namely, slip KBC, no-slip KBC and also an intermediate no-slip KBC where grain rolling and saltations are made possible by the low bed roughness. We anticipate that the shapes of the velocity profiles, observed by Sarno et al. (2018a), are only partially observed in this new campaign. In fact, owing to the increased bed slope, the lower creep flow rarely occurs. Conversely, basal grain saltations and rolling significantly influence the flow dynamics.

2. Experimental setup and measuring methods

The apparatus consists of a 2-m long Plexiglas chute with a rectangular cross section of width 8cm (i.e. ≈24 grain diameters). For all experiments the chute inclination, α, is set equal to 35°. The granular material is made of acetal-polymeric (POM) spheroidal beads with mean diameter d=3.3mm, internal angle of friction of ≈27° and coefficient of restitution of ≈0.83 (Sarno et al., 2018a). The upper part of the channel is used as a reservoir and is equipped with an external hopper (capacity 40l) (Fig. 1a). The granular material is allowed to flow down the chute through an adjustable gate, so that different flow rates could be studied. The investigated range of gate openings is from 5cm to 14cm. An intermediate steady state, lasting several seconds, was observed in all experiments.

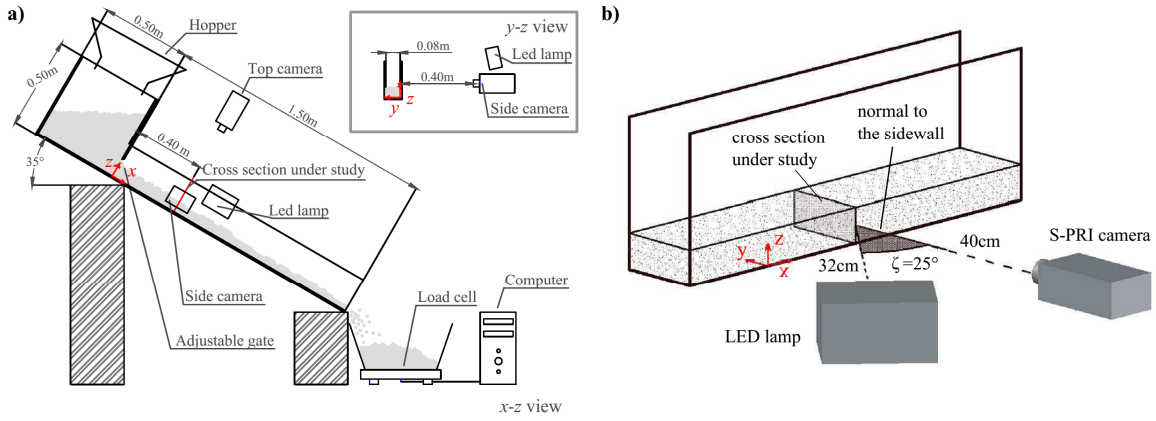

Fig. 1. (a) Experimental apparatus (chute inclination angle α=35°); (b) position of the LED lamp

Several basal surfaces with different roughness were investigated: (1) smooth Bakelite surface (S) with a characteristic length of the roughness <<10μm; (2) different sandpaper linings with characteristic lengths of the roughness of 162μm (P100 FEPA/ISO 6344), 269μm (P60), and 425μm (P40); (3) *granular* basal surface (G), made up by randomly gluing the same POM beads on the smooth bed surface (characteristic length of roughness d/2=1.65mm).

The instrumentation is composed of the following devices: a load-cell placed at the outlet for the estimation of the mass flow rate, two high-speed cameras, a high-brightness flickering-free LED lamp. The camera model AOS S-PRI was placed aside the channel to measure sidewall velocity and volume fraction at the cross section under study, located 40cm downstream the inflow gate (cf. Fig. 1). The second camera (model AOS Q-PRI) was located above

the free surface to measure the free-surface velocity profile at the same cross section (x=40cm). For reliable PIV analyses and volume fraction estimations, the cameras' sampling rate was set to 1 kHz. The LED lamp (mod. PhotoSonics MultiLED-LT) was located aside the channel at a distance of 32cm. The angle of incidence of light, ζ, with the respect to the normal to the side wall was carefully adjusted and set equal to 25° (Fig. 1b). The position of the lamp and, especially, the choice of ζ is crucial for reliable volume fraction measurements (Sarno et al., 2016).

Thanks to the open-source code PIVlab (Thielicke and Stamhuis, 2014), a window deformation multi-pass particle image velocimetry (PIV) approach is adopted for velocity measurements at the sidewall and at the free surface. In classical fluid mechanics the PIV is a well-established technique, based on the maximization of the discrete cross-correlation function between two frames delayed by a short time interval. Nonetheless, some specific measures need to be adopted to reliably extend the PIV approach to granular flows (e.g. Eckart et al., 2003; Sarno et al., 2018b). As highlighted by Sarno et al. (2018b), the employment of the window deformation approach is crucial to reduce gradient-bias errors in case of highly sheared flows, which is a frequent case in granular flows. As well, the multi-pass approach, which uses a progressive refinement of the interrogation window to obtain a high spatial resolution without loss-of-pairs errors, is particularly useful in granular flow applications. We employed the same PIV settings of Sarno et al. (2018a), to which we refer the reader for further details. According to the theoretical accuracy of PIVlab reported to be <0.02 pixel/frame (Thielicke and Stamhuis, 2014) and by also considering the specific image scales of the video-recordings, the PIV accuracy is ≈0.004 m/s and ≈0.002 m/s at the sidewall and at the free surface, respectively.

The measurement of the volume fraction is obtained by using the stochastic-optical method (SOM) proposed by Sarno et al. (2016), to which we refer the reader for details. This method, thanks to a highly-controlled illumination, allows the estimation of the near-wall volume fraction, c_{3D}, from a measurable quantity called *two-dimensional volume fraction*, c_{2D}. With reference to a given interrogation window Δ on the measuring wall, this quantity is defined as the ratio of the overall area of the projections on Δ of all the illuminated and visible surface elements belonging to the grains and the total area of Δ. A stochastic transfer function between c_{3D} and c_{2D} is found through several Monte Carlo simulations, reproducing random grain dispersions with different volume fractions

$$c_{3D} = f\left(c_{2D},\zeta\right) = a\left(\zeta\right)\exp\left(b\left(\zeta\right)c_{2D}\right), \tag{1}$$

where a and b are parameters depending on ζ. A local binarization formula, requiring the calibration of one threshold parameter, is employed for estimating c_{2D} from gray-scale images. The method was extensively validated by Sarno et al. (2016) on random dispersions of POM beads immersed in a water-sucrose solution. The best accuracy was found with angles of incidence of light, ζ, between 20° and 40°. In the present investigation we chose $\zeta = 25°$ with zero tilt of the lamp with respect to the z direction (cf. Fig. 1b). Different from Sarno et al. (2016), rectangular interrogation windows of dimensions $1d$ and $16d$ in the z and x directions, respectively, are employed. Such interrogation windows are also designed to have a 50%-overlap along z, so as to get a spatial resolution of the measurements equal to $d/2$ along the flow depth. The accuracy of the method was verified by validation on random granular dispersions of known volume fraction and a root mean square error (RMSE) on c_{3D} of ≈0.025 was obtained. Additional inaccuracies might arise near the free surface, due to the fact that the binarization algorithm struggles to identify the illuminated and visible elements whenever the background is visible. To reduce such errors, a white-noise background, with a similar brightness of POM grains but distinguishable from them, is employed.

3. Results and discussion

By comparing the experiments with the same gate opening, we preliminarily observed that the runs on different sandpaper linings always exhibit a no-slip basal KBC and very similar velocity and volume fraction profiles. It indicates that the flow dynamics is weakly influenced by changes of the basal roughness within the range [162μm, 425μm]. For brevity, we chose only to present the experiments carried out on sandpaper P40. Conversely, for ease of comparison, in Fig. 2 we report the longitudinal velocity profiles, u_x, at the sidewall, previously obtained by Sarno et al. (2018a) with α=30° and on analogous bed surfaces of those employed in the new experimental campaign (α=35°).

The list of experiments with α=35° is reported in Tab. 1. The mass flow rate, Q_m, and the flow depth, h, in Tab. 1 are obtained by two subsequent averages: the time-averages in a time interval of 1s within the steady state, are subsequently ensemble-averaged over four repetitions of the same experiment. As well, the velocity and volume fraction profiles, reported in Fig. 2 and hereafter, are obtained by time- and ensemble-averaging.

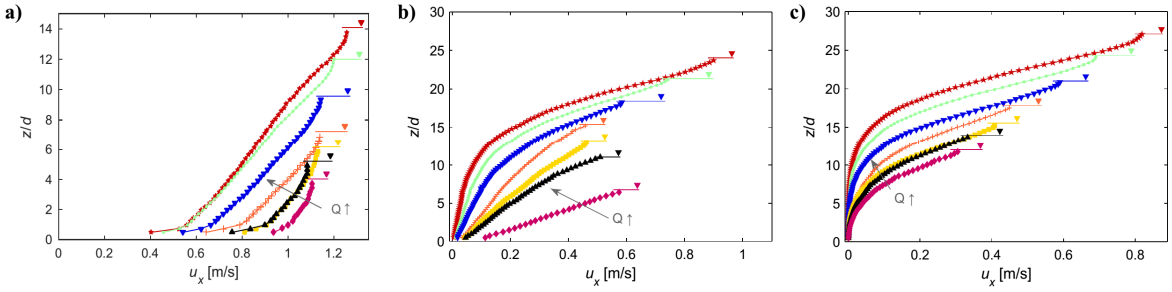

Fig. 2. Sidewall u_x velocity profiles obtained by Sarno et al. (2018a) with α=30°. (a) Bakelite (S), (b) sandpaper (P40), (c) grain surface (G)

Table 1. List of the experiments carried out by employing a chute inclination angle of 35°

Exp. ID	Gate opening [m]	Basal surface	Q_m [g/s]	h [m]
Exp-5S	0.05	Bakelite (S)	1084	0.009
Exp-6S	0.06	Bakelite (S)	1417	0.012
Exp-7S	0.07	Bakelite (S)	1725	0.016
Exp-8S	0.08	Bakelite (S)	2124	0.020
Exp-10S	0.10	Bakelite (S)	2717	0.027
Exp-12S	0.12	Bakelite (S)	3332	0.034
Exp-14S	0.14	Bakelite (S)	4243	0.044
Exp-5P40	0.05	Sandpaper (P40)	858	0.018
Exp-6P40	0.06	Sandpaper (P40)	1146	0.021
Exp-7P40	0.07	Sandpaper (P40)	1440	0.023
Exp-8P40	0.08	Sandpaper (P40)	1799	0.027
Exp-10P40	0.10	Sandpaper (P40)	2353	0.035
Exp-12P40	0.12	Sandpaper (P40)	2819	0.042
Exp-14P40	0.14	Sandpaper (P40)	3399	0.050
Exp-5G	0.05	Grain (G)	773	0.019
Exp-6G	0.06	Grain (G)	1038	0.023
Exp-7G	0.07	Grain (G)	1297	0.027
Exp-8G	0.08	Grain (G)	1555	0.031
Exp-10G	0.10	Grain (G)	2263	0.040
Exp-12G	0.12	Grain (G)	2635	0.050
Exp-14G	0.14	Grain (G)	3066	0.059

Good experimental repeatability is obtained by controlling the relative air humidity (>60%), so as to avoid significant electrostatic forces among grains and chute boundaries. The PIV measurements at the free surface showed roughly parabolic transverse velocity profiles with minima at the sidewalls, which confirms the non-negligible sidewall friction. This trend is generally observed in all experiments, regardless the bed roughness.

The runs on smooth Bakelite (*S*) exhibit a slip basal KBC with negligible grain rolling. The longitudinal velocity, u_x, and the volume fraction, c_{3D}, profiles at the sidewall are reported in Fig. 3, while the shear rate, $\partial_z u_x$, is shown in Fig. 6a. Few measurement points immediately below the free surface are chosen not to be reported in Fig. 3, since velocity and c_{3D} inaccuracies might have occurred there due to strong oscillations of the free surface. Conversely, though a further investigation is planned, we do not believe that drag effects due to air at the free surface are relevant in this experimental campaign, especially considering that the flow velocities at the free surface are relatively small (<2m/s). Due to large slip velocities, the u_x profiles are much blunter than those observed on the same S bed with α=30° (cf. Fig. 2a). By considering the additional information of the c_{3D} profiles (Fig. 3b), three regions could be

identified: (1) a ≈1d-thick region, near the basal surface, where c_{3D} is relatively small (≈0.3-0.5) and increases with z: in this region the shear rate, $\partial_z u_x$, is of order of 15-25s^{-1} (Fig. 6a) and is larger than in the rest of the flow domain; (2) an intermediate region, only noticeable if h is high enough, where c_{3D} shows an approximately constant value (slightly less than 0.6) and u_x is approximately linear with a shear rate of ≈10s^{-1} (Fig 6a); (3) a ≈2d-4d-thick upper region, where c_{3D} decreases and u_x increases less than linearly with z.

The small values of c_{3D} in the 1d-thick region near the bed are mainly caused by the fact that the fixed surface prevents grain interlocking. Conversely, the very large values of $|\partial_z c_{3D}|$, which occur near the free surface and may appear unphysical, are mainly caused by the fact that the background becomes occasionally visible due to grain saltations and, thus, the time-averaged c_{3D} rapidly decreases with z. In case of small flow depths, the u_x profile exhibits a Bagnold-like scaling (Bagnold, 1954), i.e. a 3/2-power law with z, in the entire profile, suggesting that the flow regime is mainly collisional (Sarno et al., 2018a). When h increases, the effects of the sidewall friction and, possibly, also the occurrence of non-local momentum exchanges, causes a progressive linearization of the velocity profiles, so that a convex shape of u_x can be only observed in the upper region where the flow regime is collisional and the sidewall resistances become negligible. The observed behavior of u_x is in substantial agreement with the previous experiments with α=30° (cf. Fig. 2a) and suggests the occurrence of a rheological stratification, which is further confirmed by the volume fraction measurements.

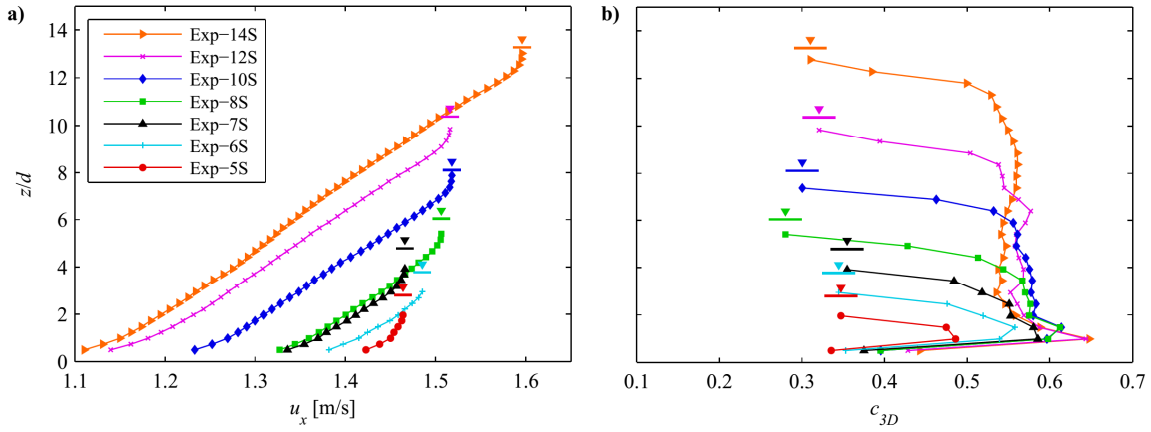

Fig. 3. Experimental profiles obtained on the smooth Bakelite bed (S). (a) Longitudinal velocity profiles, u_x; (b) volume fraction profiles, c_{3D}

Different basal KBCs were observed by increasing the basal roughness. Fig. 4 reports the experimental profiles of u_x and c_{3D}, obtained on the sandpaper bed (P40). The related shear rate profiles are shown in Fig. 6b. In this case, different from the Bakelite bed, the roughness is large enough to inhibit grain sliding: namely a no-slip KBC occurs. Yet, since the characteristic length of roughness (425μm) is still significantly smaller than the grain size, noticeable grain rolling and saltation at the basal surface are observed, especially for experiments with low h. Such phenomena are progressively inhibited by increasing h due to the increase of the normal pressures. The magnitude of grain rolling and saltation is stronger to that previously observed with α=30°. By analyzing the fluctuation velocities, it was clear that basal rolling and saltation represent a source of fluctuation kinetic energy that diffuses from z=0 toward the flow domain and, thus, increases the collisional character of the flow. As highlighted by Sarno et al. (2018a), the KBC at the bed is not only influenced by the basal angle of friction between but also by the characteristic length of the roughness, which influences the fluctuation velocities. Moreover, some influence to the fluctuation velocity at the bed could be also due to the shape of the roughness, which merits further investigation.

As a consequence, a rheological stratification slightly different from the smooth bed can be observed in Fig. 4. In the lower zone (approx. 1d-thick), c_{3D} is very small and $\partial_z u_x$ is quite high (Fig. 6b). From the lower to the central zone, c_{3D} increases for all experiments. Yet, it becomes approximately constant at ≈0.6, only in the experiments with high h (i.e. Exp-10P40, Exp-12P40 and Exp-14P40). In the same intermediate region, the u_x profiles mainly exhibit a Bagnold grain-inertial convex shape, instead of the linear shape observed on the S bed. An approximately linear behavior of u_x (cf. Fig. 6b) can be barely observed only in the three experiments with highest h. This finding can be explained by the fact that the basal roughness causes stronger grain velocity fluctuations, which propagate in the intermediate region. By comparing the experiments on sandpaper with those on smooth bed with similar h, it

emerges that such a higher grain collisionality induces a more persistent Bagnold shape of the u_x profiles. Moreover, it should be noted that the convex velocity profiles are notably different from those observed with α=30° on the same bed surface (P40), which are either linear or even concave in their lower zone (cf. Fig. 2b). This discrepancy is clearly due to the slightly different basal KBC, induced by the higher chute slope. Only if the h becomes significantly high, so that the sidewall friction increases and also the basal grain saltations are inhibited by the pressure, the character of the velocity profiles shifts from convex to approximately linear, indicating the onset of frictional mechanisms within the lower part of the flow domain. Analogous to the S bed (cf. Fig. 3), a mainly collisional layer, with a convex u_x profile and rapidly decreasing c_{3D}, takes place immediately below the free surface.

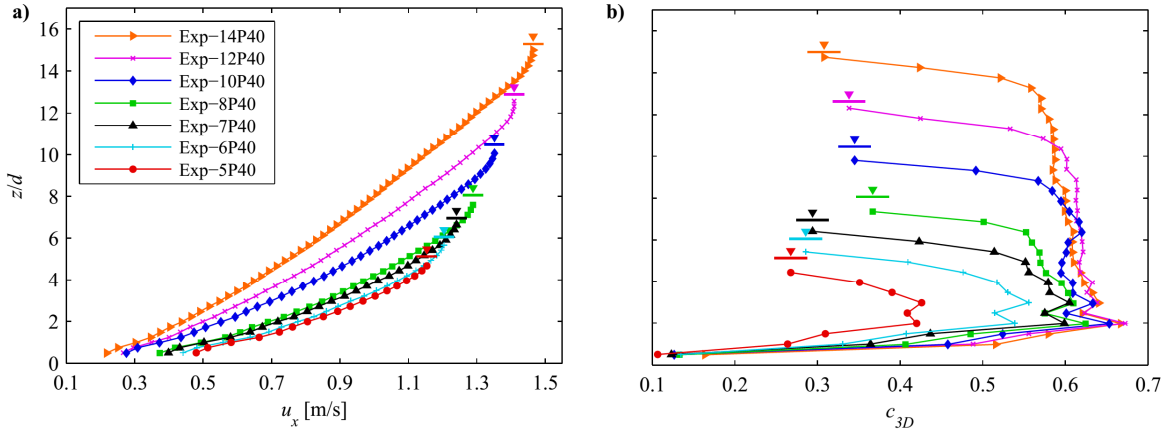

Fig. 4. Experimental profiles obtained on the sandpaper bed (P40). (a) Longitudinal velocity profiles, u_x; (b) volume fraction profiles, c_{3D}

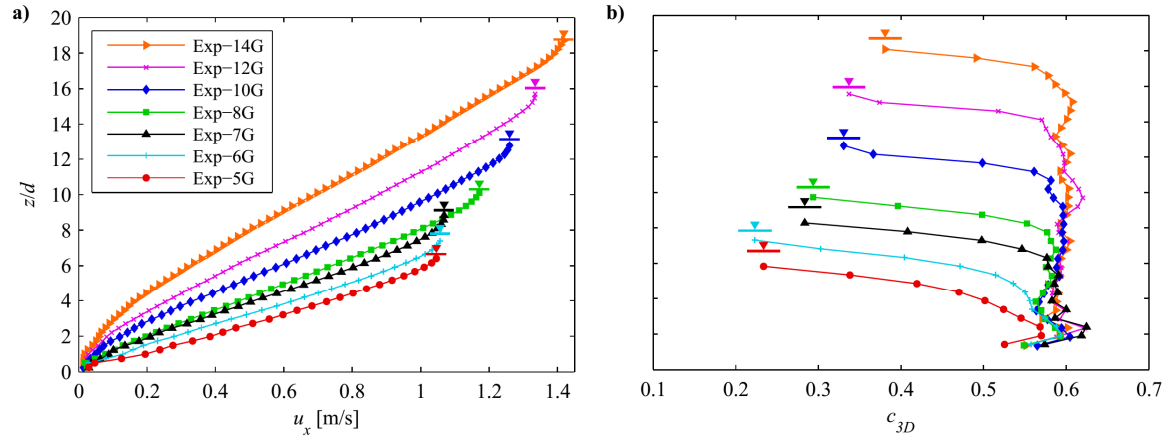

Fig. 5. Experimental profiles obtained on the grain basal surface (G). (a) Longitudinal velocity profiles, u_x; (b) volume fraction profiles, c_{3D}

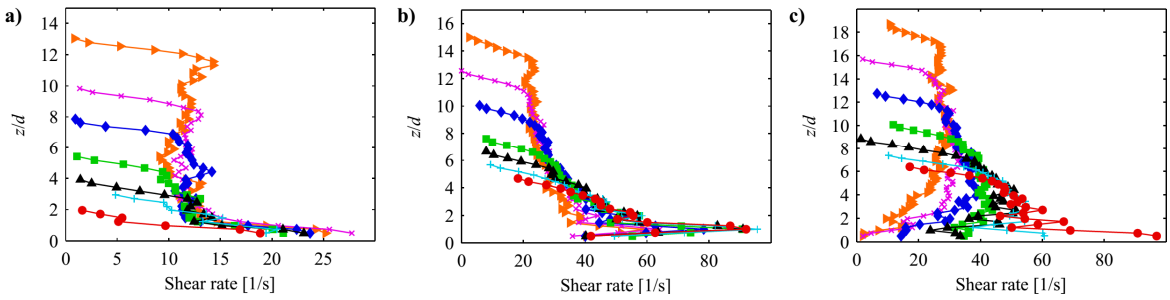

Fig. 6. Experimental profiles of the shear rate, $\partial_z u_x$. (a) smooth Bakelite (S); (b) sandpaper (P40); (c) grain basal surface (G)

Finally, the experimental results on the granular bed (G), are reported in Figs. 5 and 6c. Similar to the P40 bed, a no-slip KBC is guaranteed by the high basal friction. Yet, different from the sandpaper bed, in this case the roughness is high enough that the grain rolling and saltations are almost completely inhibited. In fact, the grains tend to interlock with the bumpy granular bed. As a consequence, a very weak grain rolling is observed only in the case of small flow depths (i.e. runs Exp-5G and Exp-6G), while in all other experiments a no-slip KBC with no rolling occurs. By comparing Fig. 5a with Fig. 2c, it can be noted that the increased chute slope does not allow the formation of a lower creep flow, characterized by very small velocities and a concave shape of the u_x profile.

Nonetheless, owing to the interlocking between the grains and the basal surface, for all experiments the volume fraction c_{3D} reaches the asymptotical value of ≈0.6 soon above the fixed bed. The c_{3D} profiles are almost constant along the entire flow depth, except near the free surface. For small enough values of h (i.e. Exp-5G, Exp-6G and Exp-7G), the shape of the u_x profile is weakly convex, analogous to the case of sandpaper bed.

When h increases, and, consequently, also the pressures and the sidewall resistances become larger, the u_x profile exhibits a progressive concave shape in its lower region and an approximately linear shape in an upper intermediate region (cf. Fig. 6c). In these cases, the behavior of the lower layer can be regarded as the onset of the creep flow regime (cf. Fig. 2c), which, however, cannot fully develop, due to the higher slope and, consequently, higher active forces. In this lower zone, frictional momentum exchanges among the grains start to become prevalent with respect to collisions, thanks to the confining effects of the normal pressures and of the sidewall resistances. Analogous to that already observed on different beds and in the experimental dataset with α=30° (Fig. 2), an upper almost collisional layer of thickness of few grain diameters, where the u_x profile shows a convex shape and c_{3D} rapidly decreases with z, occurs in all experiments on G bed. This finding suggests that the flow dynamics near the free surface is scarcely influenced by the roughness of the basal surface if h is high enough. Finally, it is worth underlining that the general shape of the c_{3D} profiles is common to all the investigated beds: near the bed $\partial_z c_{3D}>0$, while $\partial_z c_{3D}\leq 0$ along the rest of the flow depth. This finding is in agreement with other works on dry granular flows (e.g. Ancey, 2001), while it differs from some investigations on liquid-granular mixtures, where also the case $\partial_z c_{3D}>0$ was observed along the flow depth due to the other dissipation mechanisms related to the interstitial fluid (e.g. Egashira et al., 2001).

4. Conclusion

In this work we systematically studied the effects of the basal surface on the dynamics of granular flows in a rectangular chute. As an extension of the work by Sarno et al. (2018a), a higher chute inclination angle of 35° was investigated to determine the influence of larger active forces on the basal KBC. Moreover, in this experimental campaign we provided not only the flow velocity measurements but also estimations of the volume fraction by using the SOM method (Sarno et al., 2016). The comparisons of the velocity and volume fraction profiles indicate that different flow regimes coexist along the flow depth.

For all investigated basal surfaces, a Bagnold-like shape of the velocity profile is generally observed, if the flow depth is small enough. As the flow depth increases, the velocity profile becomes approximately linear in its intermediate part and, for the case of granular bed (G), even weakly convex in the lower zone. It suggests the occurrence of a rheological stratification, where the lower region is governed by frictional exchange mechanisms and the upper region is more collisional. Yet, owing to the larger bed slope with respect to the dataset reported by Sarno et al. (2018a), no fully-developed creep flow could be observed in the case of the granular bed.

In the whole dataset we observed similar behaviors of the volume fraction profiles. Small values of volume fraction occur near the fixed bed in both smooth Bakelite and sandpaper basal surface, while relatively larger values are observed in the case of the bumpy grain bed. In the regions where the velocity profiles exhibit a convex shape, the volume fraction is typically smaller than 0.6. Conversely, the volume fraction is found to exhibit an approximately constant value close to ≈0.6, where a linear velocity profile occurs. In the experiments on sandpaper beds, interestingly, we observed that the Bagnold convex shape of the velocity profiles persists also in the presence of relatively high flow depths. This finding seems to be due to grain rolling and saltations at the basal surface, made possible by the roughness much smaller than the grain diameter and by the increased acting forces, in turn due to the larger bed slope. Such a complex no-slip KBC, allowing basal grain rolling and saltations, seems responsible for an increase of the grain collisionality also in the upper regions of the flow domain. Immediately below the free surface, a prevalently collisional layer with rapidly decreasing volume fraction and convex velocity profiles is observed in all experiments, independent from the kind of basal surface.

From these experimental findings it emerged that the granular flow dynamics and the occurrence of stratified flow regimes depend on the basal roughness and sidewall resistances but it is also crucially governed by the active forces due to the bed slope. Further laboratory investigations with larger bed slopes and on bed surfaces with intermediate roughnesses could be useful to better understand the flow regimes, and, the behavior of the fluctuation velocities at the bed. Moreover, a further investigation on the scale effects of this laboratory study, especially those ones due to rate-dependent dissipations, could be useful to extend the experimental findings to field-scale applications.

Acknowledgements

The authors thank V. D'Avino for help in the experimental campaign given during his traineeship at the University of Salerno. The authors are also grateful to N. Immediata for valuable assistance in experimental design.

References

Ancey, C., 2001, Dry granular flows down an inclined channel: Experimental investigations on the frictional-collisional regime: Physical Review E, v. 65, no. 1, 011304, doi:10.1103/PhysRevE.65.011304.

Armanini, A., Capart, H., Fraccarollo, L., and Larcher, M., 2005, Rheological stratification in experimental free-surface flows of granular–liquid mixtures: Journal of Fluid Mechanics, v. 532, p. 269-319, doi:10.1017/S0022112005004283.

Bagnold, R. A., 1954, Experiments on a gravity-free dispersion of large solid spheres in a Newtonian fluid under shear: Proceedings of the Royal Society A, v. 225, no. 1160, p. 49-63, doi:10.1098/rspa.1954.0186.

Baker, J., Gray, N., and Kokelaar, P., 2016, Particle size-segregation and spontaneous levee formation in geophysical granular flows: International Journal of Erosion Control Engineering, v. 9, no. 4, p. 174-178, doi:10.13101/ijece.9.174.

Eckart, W., Gray, J.M.N.T., and Hutter, K., 2003, Particle Image Velocimetry (PIV) for granular avalanches on inclined planes, *in* Hutter, K., Kirchner, N., eds., Dynamic response of granular and porous materials under large catastrophic deformations: Lecture notes in applied and computational mechanics, v. 11, Springer, Berlin, p. 195-218, doi:10.1007/978-3-540-36565-5_6.

Egashira, S., Itoh, T., and Takeuchi, H., 2001, Transition mechanism of debris flows over rigid bed to over erodible bed: Physics and Chemistry of the Earth, Part B: Hydrology, Oceans and Atmosphere, v. 26, no. 2, p. 169-174, doi:10.1016/S1464-1909(00)00235-5.

Iverson, R. M., and Vallance, J. W., 2001, New views of granular mass flows: Geology, v. 29, no. 2, p. 115-118. doi:10.1130/0091-7613(2001)029<0115:NVOGMF>2.0.CO;2.

Iverson, R. M., and George, D. L., 2014, A depth-averaged debris-flow model that includes the effects of evolving dilatancy. I. Physical basis: Proceedings of the Royal Society A, v. 470, no. 2170, 20130819, doi:10.1098/rspa.2013.0819.

Jesuthasan, N., Baliga, B. R., and Savage, S. B., 2006, Use of particle tracking velocimetry for measurements of granular flows: review and application: KONA Powder and Particle Journal, v. 24, p. 15-26, doi:10.14356/kona.2006006.

Jop, P., Forterre, Y., and Pouliquen, O., 2005, Crucial role of sidewalls in granular surface flows consequences for the rheology: Journal of Fluid Mechanics, v. 541, p. 167-192, doi:10.1017/S0022112005005987.

Kuo, C. Y., Tai, Y. C., Bouchut, F., Mangeney, A., Pelanti, M., Chen, R. F., and Chang, K. J., 2009, Simulation of Tsaoling landslide, Taiwan, based on Saint Venant equations over general topography: Engineering Geology, v. 104, no. 3-4, p. 181-189, doi:10.1016/j.enggeo.2008.10.003.

Medina, V., Hürlimann, M., and Bateman, A., 2008, Application of FLATModel, a 2D finite volume code, to debris flows in the northeastern part of the Iberian Peninsula: Landslides, v. 5, no. 1, p. 127-142, doi:10.1007/s10346-007-0102-3.

MiDi, G. D. R., 2004, On dense granular flows: European Physical Journal E, 14(4), 341-365, doi:10.1140/epje/i2003-10153-0.

Mills, P., Loggia, D., and Tixier, M., 1999, Model for a stationary dense granular flow along an inclined wall: Europhysics Letters, v. 45, no. 6, 733, doi:10.1209/epl/i1999-00229-y.

Papa, M., Sarno, L., Vitiello, F., and Medina, V., 2018, Application of the 2D Depth-Averaged Model, FLATModel, to Pumiceous Debris Flows in the Amalfi Coast: Water (Switzerland), v. 10, no. 9, 1159, doi:10.3390/w10091159.

Pouliquen, O., and Forterre, Y., 2009, A non-local rheology for dense granular flows: Philosophical Transactions of the Royal Society A, v. 367. no. 1909, p. 5091-5107, doi:10.1098/rsta.2009.0171.

Sarno, L., Papa, M.N., and Martino, R., 2011a, Dam-break flows of dry granular material on gentle slopes, *in* Proceedings of the 5th International Conference on Debris-Flow Hazards Mitigation, Padua, Italy, June 2011, p. 503-512, doi:10.4408/IJEGE.2011-03.B-056.

Sarno, L., Martino, R., and Papa, M. N., 2011b, Discussion of ''Uniform flow of modified bingham fluids in narrow cross sections'' by A. Cantelli: Journal of Hydraulic Engineering, v. 137, no. 5, p. 621, doi:10.1061/(ASCE)HY.1943-7900.0000238.

Sarno, L., Carravetta, A., Martino, R., and Tai, Y.-C., 2014, A two-layer depth-averaged approach to describe the regime stratification in collapses of dry granular columns: Physics of Fluids, v. 26, no. 10, p. 103303, doi:10.1063/1.4898563.

Sarno, L., Papa, M.N., Villani, P., and Tai, Y.-C., 2016, An optical method for measuring the near-wall volume fraction in granular dispersions: Granular Matter, v. 18, no. 4, doi:10.1007/s10035-016-0676-3.

Sarno, L., Carravetta, A., Martino, R., Papa, M. N., and Tai, Y. C., 2017, Some considerations on numerical schemes for treating hyperbolicity issues in two-layer models: Advances in water resources, v. 100, p. 183-198, doi:10.1016/j.advwatres.2016.12.014.

Sarno, L., Carleo, L., Papa, M.N., and Villani, P., 2018a, Experimental investigation on the effects of the fixed boundaries in channelized dry granular flows: Rock Mechanics and Rock Engineering, v. 51, no. 1, p. 203-225, doi:10.1007/s00603-017-1311-2.

Sarno, L., Carravetta, A., Tai, Y.-C., Martino, R., Papa, M.N., and Kuo, C.-Y, 2018b, Measuring the velocity fields of granular flows – Employment of a multi-pass two-dimensional particle image velocimetry (2D-PIV) approach: Advanced Powder Technology, v. 29, no. 12, p. 3107-3123, doi:10.1016/j.apt.2018.08.014.

Thielicke, W., and Stamhuis, E.J., 2014, PIVlab–Towards user-friendly, affordable and accurate digital particle image velocimetry in MATLAB: Journal of Open Research Software, v. 2, no.1, doi:10.5334/jors.bl.